Frontiers in Bioscience Landmark

Front. Biosci. (Landmark Ed) **2026**; 31(8): 52899
https://doi.org/10.31083/FBL52899

Original Research

Association of c-Myc and Immune Cell Infiltration in Small Cell Lung Carcinoma

Peiyan Zhao[1,2], Hui Li[1,2], Xinyue Wang[1,2], Na Di[3], Yan Liu[1,2], Lin Tian[1,2], Rui Zhong[1,2], Changlin Liang[1,2], Haifeng Liu[1,2,*]

[1]Translational Oncology Research Lab, Jilin Cancer Hospital, 130000 Changchun, Jilin, China
[2]Jilin Provincial Key Laboratory of Molecular Diagnostics for Malignant Tumor, Jilin Cancer Hospital, 130000 Changchun, Jilin, China
[3]Biobank, Jilin Cancer Hospital, 130000 Changchun, Jilin, China
*Correspondence: hflydw@163.com (Haifeng Liu)
Academic Editor: Sung Eun Kim
Submitted: 14 April 2026 Revised: 30 May 2026 Accepted: 16 June 2026 Published: 13 August 2026

Abstract

Background: Small cell lung carcinoma (SCLC) is a highly aggressive, rapidly proliferating malignancy largely corresponding to immune-cold tumor type. The role of the key oncogene c-Myc in regulating the complex immune microenvironment of SCLC remains unknown. **Methods:** Immunohistochemistry and multiplex immunofluorescence techniques were used to analyze c-Myc expression and immune cell infiltration. c-Myc and β-catenin expression were analyzed using western blotting. Flow cytometry was used to quantify the expression of immunosuppressive ligands—including programmed death ligand 1 (PD-L1), CD47, CD155, and human leukocyte antigen-E (HLA-E)—and characterize the function of T cells and macrophages. Cytokine levels were evaluated using enzyme-linked immunosorbent assays. **Results:** c-Myc expression in high tumor-infiltrating lymphocyte infiltration (TIL^{high}) tumor exceeded that in TIL^{low} tumors (n = 24) and was positively correlated with $CD163^{+}$ macrophage infiltration (p = 0.0180). Immunosuppressive ligands were universally expressed on SCLC cells. 10058-F4—a c-Myc inhibitor—substantially downregulated the expression of PD-L1, CD47, and CD155 and upregulated HLA-E expression. In the coculture system, the inhibition of c-Myc in SCLC cells significantly upregulated interferon-gamma production in Jurkat cells, inhibited macrophage phagocytosis, and decreased cytokine concentrations in the supernatant. Further mechanistic studies revealed that c-Myc inhibition modulated the Notch signaling pathway and reduced the expression of E-cadherin, vascular endothelial (VE)-cadherin, and β-catenin. A β-catenin agonist improved the regulatory effect of 10058-F4 on the immunosuppressive ligands in SCLC cells. **Conclusions:** c-Myc expression in SCLC is associated with immune infiltration and may regulate the expression of immune-related ligands on SCLC cells via WNT/β-catenin signaling.

Keywords: small cell lung carcinoma; immunity; macrophage; ligand

1. Introduction

Of all cancers, lung cancer has the highest incidence and mortality rates [1]. Small cell lung Carcinoma (SCLC) accounts for only 13%–15% of lung cancers but is considered a refractory malignancy because of its rapid progression and early metastasis [2,3]. In clinical practice, according to the system of the United States Veterans Administration, SCLC is classified into limited-stage SCLC (LS-SCLC) and extensive-stage SCLC (ES-SCLC). In the former case, the disease is confined to one hemithorax—where the primary tumor and regional lymph nodes can be adequately encompassed within a single radiation field—without additional intrathoracic metastasis. In the latter case, the disease cannot be classified as limited-stage and involves pleural, pericardial, or distant metastasis [4]. ES-SCLC accounts for two-thirds of SCLC cases and has a five-year survival rate of <2% [5]. The emergence of immune checkpoint therapy has significantly prolonged the survival of patients with ES-SCLC and changed the SCLC treatment landscape [6,7]. However, the beneficiary population and response period of patients with SCLC remain limited because of the lack of predictive biomarkers for SCLC immunotherapy. A comprehensive understanding of the characteristics and regulatory mechanisms of the SCLC immune microenvironment may provide new insights for clinical practice and translational research.

c-Myc is a protooncogene that functions as a universal transcriptional amplifier by interacting with numerous factors and complexes regulating almost every cellular process [8]. In addition to being associated with genomic instability, c-Myc is involved in the recruitment of elements in the tumor microenvironment, making the stroma more suitable for tumor cell progression, facilitating immune evasion, and promoting tumor growth into more aggressive and metastatic phenotypes [9]. In SCLC, c-Myc activates the Notch signaling pathway to dedifferentiate neuroendocrine (NE) tumor cells and promotes the temporal evolution of SCLC into a subtype with immune infiltration [10], thus being a predictive biomarker for SCLC immunotherapy. In a cohort of 135 ES-SCLC patients receiving chemotherapy alone or in combination with immune checkpoint inhibitors (ICIs), the tumors were stratified into noninflamed

and inflamed groups, with higher *MYC* gene expression observed in the former case ($p = 0.02$). In the chemotherapy + ICI cohort ($n = 39$), patients with low MYC expression exhibited longer median progression-free survivals (PFS) (5.3 vs. 4.0 months, $p = 0.028$, hazard ratio (HR) = 2.18) and higher 12-month PFS rates (23.5% vs. 4.6%) than those with high MYC expression, whereas no such difference was observed in the chemotherapy-only cohort ($n = 50$) ($p = 0.77$, HR = 1.09) [11]. The oncogenic activation of MYC was reported to impair interferon-gamma (IFN-γ)-mediated transcriptional activation by downregulating JAK2 in lung cancer [12]. Moreover, c-Myc was found to regulate the expression of NKG2DL in SCLC cells through histone deacetylase 3 (thereby modulating the killing function of natural killer (NK) cells [13]) and promote the protumor phenotype of macrophages by inducing hypersialylation [14]. Thus, the regulatory mechanisms of c-Myc and its relationship with the infiltration and function of immune cells should be investigated further.

Herein, we analyzed tumor samples from patients with SCLC to determine the relationship between c-Myc expression and immune cell infiltration. Moreover, we examined the regulatory mechanism of c-Myc and its effect on SCLC cells and the expression of various immune-related ligands, including programmed death ligand 1 (PD-L1), CD47, human leukocyte antigen-E (HLA-E), and CD155, as well as the immune regulator of c-Myc in SCLC, to provide evidence for studying the biomarkers of SCLC immunotherapy and identifying new immunotherapy targets.

2. Materials and Methods

2.1 Tissue Microarray (TMA)

c-Myc expression was studied using a TMA containing 24 primary tumors from 24 patients with LS-SCLC (R024Lu01; Zhongke Guanghua bioaitech company, Xi'an, Shaanxi, China). Tissues were fixed in 4% buffered formalin and then embedded in paraffin. The tissue spot diameter was 1.5 mm. Informed patient consent was obtained prior to tissue collection. All procedures complied with the relevant regulations and the Declaration of Helsinki.

2.2 Cell Culturing

Human SCLC cell lines SHP-77, NCI-H1092 (H1092), SCLC-21H (21H), NCI-H446 (H446), and NCI-H2227 (H2227), human lung epithelial cell line Beas-2B, human acute T lymphocyte leukemia cell line Jurkat, and human monocyte leukemia cell line THP-1 (American Type Culture Collection, Manassas, VA, USA) were maintained at 37 °C in RPMI-1640 or high-glucose Dulbecco's Modified Eagle Medium with 10 vol% FBS and antibiotics (100 IU/mL of penicillin and streptomycin). All cell lines were validated by STR profiling, tested negative for mycoplasma, and cultured in a humidified incubator under 5% CO_2 in air. Cells at passage 3 to 6 were used in this study.

2.3 Multiplex Immunofluorescence

The TMA was baked for 1 h at 63 °C and dewaxed using an automatic dyeing machine (Leica ST5020, Leica, Germany). After antigen retrieval, the slides were treated with H_2O_2 for 10 min, washed with Tris-buffered saline with 0.05% Tween-20 (TBST), and incubated with a blocking buffer for 10 min and then with the primary CD56 mouse antibody (3576, Cell Signaling Technology, USA, 1:100) at room temperature for 1 h. The slides were washed with TBST, incubated with the secondary antibody for 10 min at room temperature, and washed again with TBST. The slides were dropwise treated with the Opal dye dilution and incubated for 10 min at room temperature. After washing with TBST, the slides were repaired using a microwave oven. The other markers were stained, and the blocking and incubation with primary and secondary antibodies were repeated until all markers were labeled. The antibodies were stained in the following order: FOXP3 mouse antibody (320202, BioLegend, USA, 1:100), CD163 rabbit antibody (93498, CST, USA, 1:200), CD8A mouse antibody (70306, CST, USA, 1:200), and panCK mouse antibody (C2562, Sigma, USA, 1:1000). The slides were incubated with DAPI (G1407, Servicebio, China) for 5 min at room temperature and washed with TBST. After mounting with VECTASHIELD® HardSet Antifade Mounting Medium (H-1400, Vector Labs), the slides were scanned and analyzed using the Olympus OlyVIA software 2.9.1 (Olympus Corporation, Münster, Germany). The sum of the ratios of $CD163^+$ and $CD8^+$ cells was used as an indicator to evaluate the degree of tumor-infiltrating lymphocyte (TIL) infiltration. The median value (0.103735231) was used to define TIL^{high} (≥0.103735231) and TIL^{low} (<0.103735231) groups (**Supplementary Table 1**).

2.4 Immunohistochemistry

The TMA was baked at 63 °C for 1 h, dewaxed in a graded ethanol series and xylene, and subjected to antigen retrieval. After blocking, the slides were incubated with rabbit antihuman c-Myc antibody (ab32072, Abcam, UK, 1:50) overnight at 4 °C, rewarmed, and washed with PBS buffer. Blocking, secondary antibody binding, and DAB chromogenic procedures were performed using an automated immunohistochemistry instrument (Autostainer Link 48, Dako) and followed by counterstaining with hematoxylin for 1 min. The TMA was mounted using neutral resin and imaged under a microscope. c-Myc expression was categorized as negative (0) or positive with semiquantitative scoring for intensity (1 = weak, 2 = moderate, 3 = strong) and percentage of stained cells (1%–100%) using light microscopy. The product of the intensity score and stained cell percentage yielded a histoscore (H-score) ranging from 0 to 300.

2.5 Western Blotting

Western blotting was performed as described elsewhere [15]. Cells were lysed in RIPA buffer containing 1 mM phenylmethylsulphonyl fluoride and centrifuged at 15,000 *g* for 15 min at 4 °C. The protein concentration of the supernatant was determined using the Enhanced BCA Protein Assay Kit (P0010, Beyotime, Shanghai, China). Proteins (30 μg) were separated by sodium dodecyl sulfate polyacrylamide gel electrophoresis, transferred to polyvinylidene fluoride membranes (Millipore, Billerica, MA, USA), blocked with skimmed milk, and incubated overnight at 4 °C with primary antibodies in 5% skimmed milk. After washing with TBST, the membranes were incubated with secondary antibodies for 1 h at room temperature. The blots were examined using chemiluminescence (P0018AM, Beyotime, Shanghai, China), with images analyzed using the Image J software v1.8.0 (National Institutes of Health, Bethesda, Maryland, USA). The following antibodies were used: GAPDH (1:50,000) (WL01114, Wanleibio, Shenyang, China), Notch1 (1:1000) (3068, CST, USA), cleaved Notch 1 (1:1000) (4147, CST, USA), RBPSUH (1:1000) (5313, CST, USA), MAML1 (1:1000) (12166, CST, USA), c-Myc (1:1000) (5605, CST, USA), p21 (1:1000) (2947, CST, USA), HES1 (1:1000) (11988, CST, USA), cyclin D3 (1:1000) (2936, CST, USA), β-catenin (1:1000) (WL0962a, Wanleibio, Shenyang, China), E-cadherin (1:1000) (WL01482, Wanleibio, China), VE-cadherin (1:1000) (WL02033, Wanleibio, China), and horseradish peroxidase–conjugated goat antirabbit IgG (1:3000) (7074, CST, USA) and horse antimouse IgG (1:1000) (7076, CST, USA).

2.6 Inhibitor or Agonist Incubation

Beas-2B, H446, and SHP-77 cells were cocultured with 10058-F4 (SC6650, Beyotime, Shanghai, China), SKL2001 (HY-101085, MedChemExpress, Italy), or 10058-F4 combined with SKL2001 for 48 h and collected for the following studies.

2.7 Flow Cytometry

The cultured cells were harvested, washed twice with PBS containing 2% FBS, and stained with PE-labelled mouse antihuman HLA-E (566921, BD Pharmingen, USA), FITC-labelled mouse antihuman CD47 (556045, BD Pharmingen, USA), PE-labelled PD-L1 (329706, BioLegend, USA), Alexa Fluor® 647–labelled mouse antihuman CD155 (566305, BD Pharmingen, USA), or PE-labelled mouse IgG2a κ isotype ctrl antibody (400212, BioLegend, USA) with 5 μL/test on ice in the dark for 30 min. After staining, the cells were washed twice with PBS containing 2% FBS and analyzed using a flow cytometer (FACSCanto II, BD, USA). We first gated total cells on FSC/SSC dot plots. Doublets were excluded via FSC-A versus FSC-H gating. Live cells were gated by forward and side scatter. Fluorescence compensation was calibrated with single-color stained cells. Isotype controls were applied to define positive gates for each marker. Complete hierarchical gating procedures were performed to analyze target cell populations. Data were processed using the FlowJo software v10 (BD Biosciences, Ashland, OR, USA).

2.8 Coincubation of SCLC Cells With T Cells

Beas-2B and SCLC cells (5×10^5 cells/well), including untreated and 10058-F4-treated groups, were seeded in 12-well plates and cultured overnight. Jurkat cells were then added (SCLC:Jurkat = 1:10) without 10058-F4. After 48 h, the supernatants and cocultured cells were harvested for enzyme-linked immunosorbent assay (ELISA) and flow cytometry, respectively.

2.9 Enzyme-Linked Immunosorbent Assay (ELISA)

The concentration of IFN-γ in the medium for the coincubation of Jurkat cells with Beas-2B and SCLC cells with or without 10058-F4 treatment was determined using a human IFN-γ ELISA kit (EK180-96, MULTI SCIENCE, China). Human interleukin (IL)-6, IL-10, and granulocyte-macrophage colony-stimulating factor (GM-CSF) ELISA kits (EK106-96, EK110-96, EK-163-96, MULTI SCIENCE, China) were used to detect the corresponding concentrations in the medium used for the coincubation of macrophages with SCLC cells. After soaking and patting dry, the strips were sequentially treated with the standard and culture supernatant (100 μL/well) and a freshly prepared detection antibody solution (1:100 dilution, 50 μL/well) and incubated at room temperature with shaking (100–300 rpm) for 2 h after sealing. The strips were subsequently washed six times with 1× washing solution and patted dry. After sealing, diluted horseradish peroxidase-labeled streptavidin (1:100 dilution, 100 μL/well) was added and incubated at room temperature with shaking (100–300 rpm) for 45 min. After washing six times and patting dry, each well was supplemented with 100 μL of chromogenic substrate (TMB), incubated at room temperature for 5–30 min in the dark, and supplemented with 100 μL of the stop solution. A microplate reader was used for dual-wavelength detection within 30 min, and optical density (OD) was determined at the maximum absorption wavelength of 450 nm and reference wavelength of 630 nm. The difference between the former and latter values was used as calibrated OD.

2.10 Macrophage Differentiation

THP-1 cells (5×10^5 cells/well) were seeded in 12-well plates and differentiated into macrophages by incubation with 5 ng/mL phorbol 12-myristate 13-acetate (Sigma-Aldrich, USA) for 48 h and then with lipopolysaccharide (Sigma-Aldrich, USA) for 24 h. After incubation, the cells were stained using PKH67 (HY-D1421, MCE, USA) according to the manufacturer's protocol. Briefly, 10^6 cells were incubated with 100 μL of a 250-fold diluted working

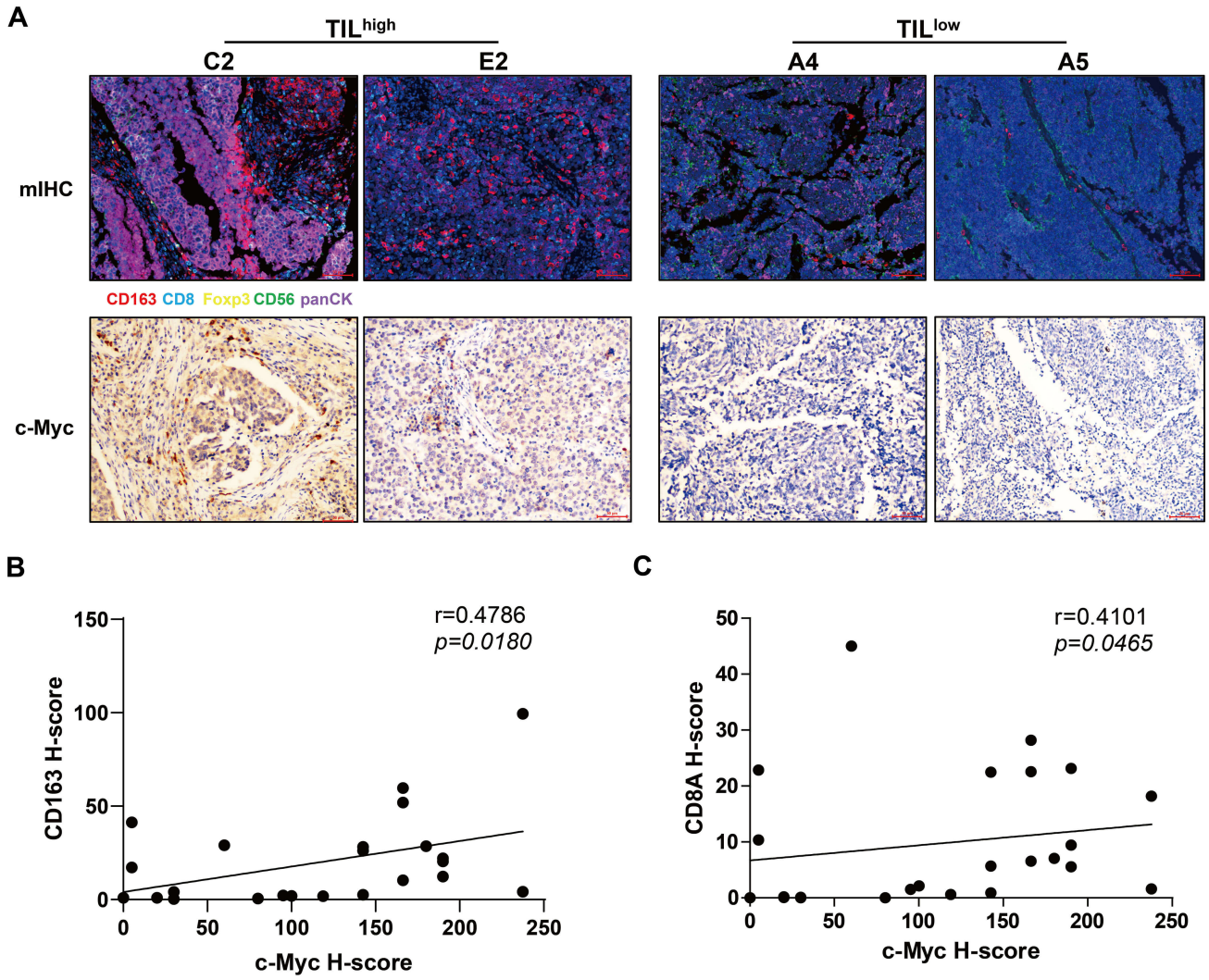

Fig. 1. Correlation between c-Myc expression and TIL infiltration in SCLC tissues. (A) Multiplex immunofluorescence and immunohistochemistry results for representative samples in TIL^{high} and TIL^{low} groups. Scale bar = 50 µm. Correlations between (B) CD163 and c-Myc H-scores (n = 24 for biological duplication) and (C) CD8A and c-Myc H-scores (n = 24 for biological duplication). The correlations between the CD163 H-score or CD8A H-score and c-Myc H-score were analyzed using Spearman's correlation analysis. TIL, tumor-infiltrating lymphocyte; SCLC, small cell lung carcinoma.

solution at 37 °C for 5 min and then at 4 °C for 15 min, centrifuged at 1000 g for 5 min, and then washed twice with PBS.

2.11 Coincubation of SCLC Cells With Macrophages

Beas-2B and SCLC cells were labeled with Vybrant™ DiD Cell-Labeling Solution (V22887, Invitrogen, USA). Briefly, the cells were suspended in serum-free 1640 medium at 1 × 10^6 cells/mL, mixed with 5 µL/mL labeling solution, incubated at 37 °C for 20 min, and centrifuged at 1000 g for 5 min, with the supernatant discarded. The cells were gently resuspended in prewarmed medium and washed at least twice. The labeled Beas-2B and SCLC cells were then counted and cocultured with macrophages at a 1:5 ratio. Phagocytosis percentage was assessed by flow cytometry after 48 h.

2.12 Statistical Analysis

All experiments were carried out using three independent replicates. The Shapiro-Wilk test was adopted to test the normality of all continuous measurement data before statistical analysis. For normally distributed continuous variables, the results were presented as means ± standard deviations. One-way analysis of variance (ANOVA) with post-hoc multiple comparisons was used for comparisons among three or more groups, while student's two-tailed t-test was was applied to compare two groups. Correlations between the CD163 H-score or CD8A H-score and the c-Myc H-score were analyzed using Spearman's correlation analysis. $p < 0.05$ was considered statistically significant. Data were analyzed using the GraphPad Prism software (version 8.0) (GraphPad Software, San Diego, CA, USA).

Table 1. Correlation between c-Myc expression and clinicopathological characteristics in SCLC.

	Variables	c-Myc expression			*p*	*r*
		Low	High	Total		
Sex	Male	4	1	5	0.317	0.308
	Female	8	11	19		
Age	≤54	7	5	12	0.684	0.167
	>54	5	7	12		
T	I–II	7	10	17	0.371	−0.275
	III	5	2	7		
N	N0	4	6	10	0.680	−0.169
	N1/N2/N3	8	6	14		
M	M0	11	12	23	1.000	−0.209
	M1	1	0	1		
Tumor size	≤4 cm	5	7	12	0.684	−0.129
	>4 cm	6	5	11		
TNM	I–II	6	9	15	0.400	−0.258
	III–IV	6	3	9		
LNM	Existent	4	6	10	0.680	−0.169
	Nonexistent	8	6	14		
Pathological type	SCLC	10	8	18	0.640	0.192
	C-SCLC	2	4	6		
TILs	Low	9	3	12	0.039*	0.500
	High	3	9	12		

* significant difference. TNM, tumor/node/metastasis; LNM, lymph nodes metastasis.

3. Results

3.1 Correlation Between c-Myc Expression in SCLC Tumor Tissues and Immune Cell Infiltration

Owing to the difficulty in obtaining a sufficient amount of ES-SCLC tissue for molecular analysis, we employed a TMA derived from 24 LS-SCLC patients to assess the expression of c-Myc, CD163, CD8, Foxp3, CD56, and panCK in tumor tissues and thus determine whether c-Myc expression in SCLC is associated with immune cell infiltration. The H-score was used to quantify the expression of each marker. The histologic characteristics of the TMA are detailed in **Supplementary Table 2**. The average patient age was 53.33 (standard deviation: 10.11), and the male-to-female ratio was 1:3.8. $CD163^+$ macrophages and $CD8^+$ T cells were found to infiltrate SCLC tissues. The sum of $CD163^+$ and $CD8^+$ cell counts divided by the total cell count was used as an indicator of the degree of TIL infiltration [16], and the cutoff was determined as the median value (**Supplementary Table 1**). c-Myc expression in TIL^{high} tumors exceeded that in TIL^{low} tumors (Fig. 1A). TIL infiltration was significantly correlated with c-Myc expression (Table 1, $p = 0.039$), and the CD163 H-score was positively correlated with the c-Myc H-score (Fig. 1B, $p = 0.0180$). The correlation between the CD8A and c-Myc H-scores was not as strong (Fig. 1C, $p = 0.0465$), which implied that c-Myc expression was positively correlated with immune cell infiltration, especially with the degree of infiltration by $CD163^+$ macrophages.

3.2 Regulatory Effect of c-Myc on the Expression of Immune-Related Ligands in SCLC Cells

Common immunosuppressive ligands in tumors include PD-L1, CD47, CD155, and HLA-E, and the corresponding receptors are PD-1, signal regulatory protein α (SIRPα), T cell immunoreceptor with Ig and ITIM domains (TIGIT), and NKG2A, respectively. These ligands cause the transmission of inhibitory signals and inhibit the function of T cells, macrophages, and NK cells. To investigate the regulatory effect of c-Myc on the expression of these inhibitory ligands in SCLC, we measured the expression level of c-Myc in different SCLC cells and Beas-2B cells, revealing that all six cells expressed c-Myc (Fig. 2A). SHP-77 and H446 cells, which are commonly used for *in vitro* studies and represent A and N subtypes, respectively [17], were selected for further investigation, as these two subtypes collectively constitute ~70% of SCLC cells and thus represent the majority of cases [18]. Beas-2B, H446, or SHP-77 cells were treated with different concentrations of c-Myc inhibitor 10058-F4. c-Myc expression was suppressed at 5 μM 10058-F4 in Beas-2B and H446 cells and at 80 μM in SHP-77 cells (Fig. 2B–D). Therefore, the working concentration of 10058-F4 was chosen as 5 μM in Beas-2B and H446 cells and 80 μM in SHP-77 cells.

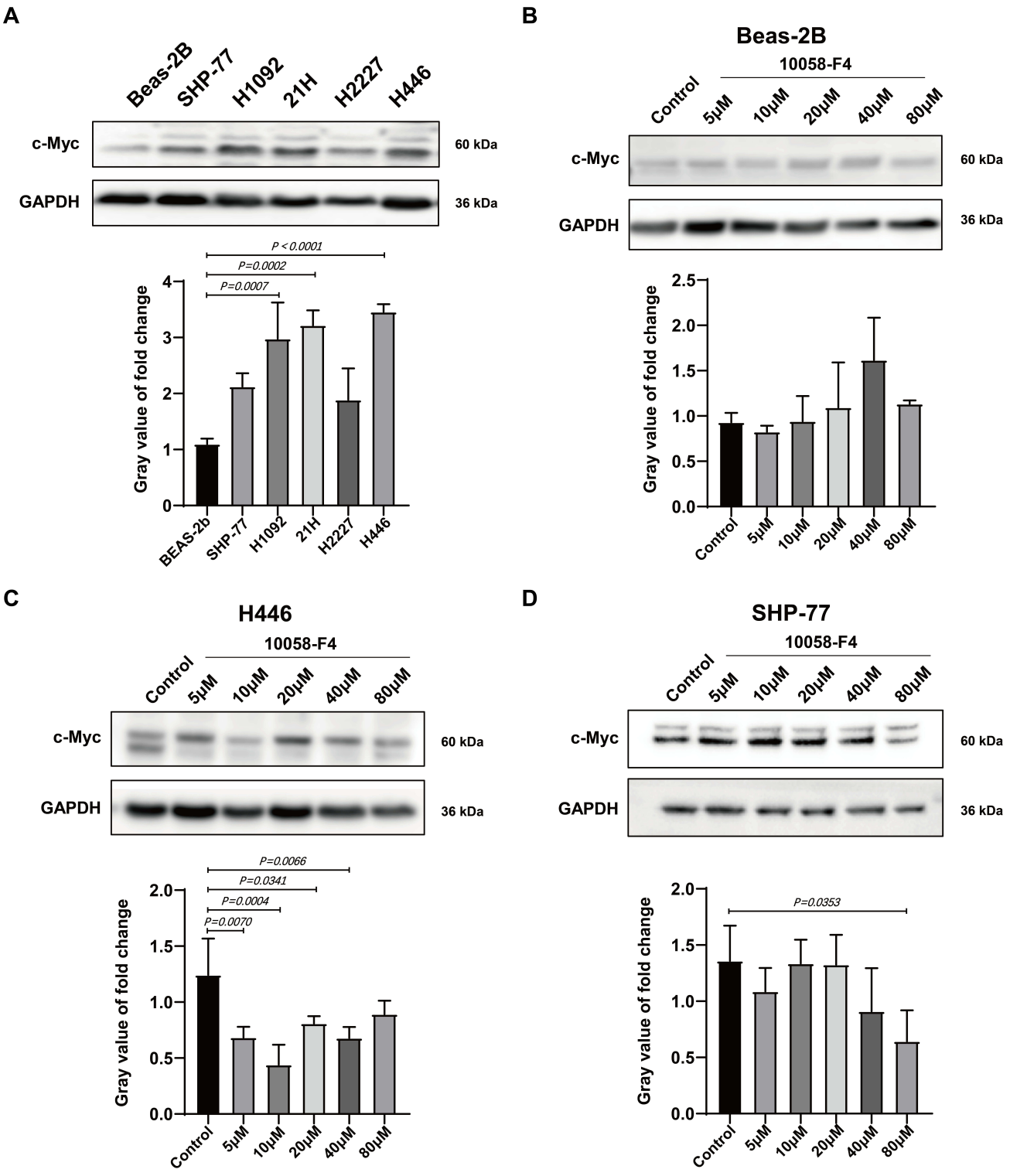

Fig. 2. Expression of c-Myc and inhibition of 10058-F4 in SCLC cells. c-Myc expression level in (A) untreated Beas-2B, SHP-77, H1092, 21H, H2227, and H446 cells and (B) Beas-2B, (C) H446, and (D) SHP-77 cells treated with different concentrations of 10058-F4. GAPDH, glyceraldehyde-3-phosphate dehydrogenase.

The mean fluorescence intensity (MFI) of PD-L1, CD47, CD155, and HLA-E was determined on the surface of Beas-2B, H446, SHP-77, H2227, and H1092 cells and found to be highest for CD155 (Fig. 3A). 10058-F4 significantly downregulated CD155 expression on the surface of H446 and SHP-77 cells while downregulating PD-L1 and CD47 expression and upregulating HLA-E expression on the surface of SHP-77 cells (Fig. 3B). However, the expres-

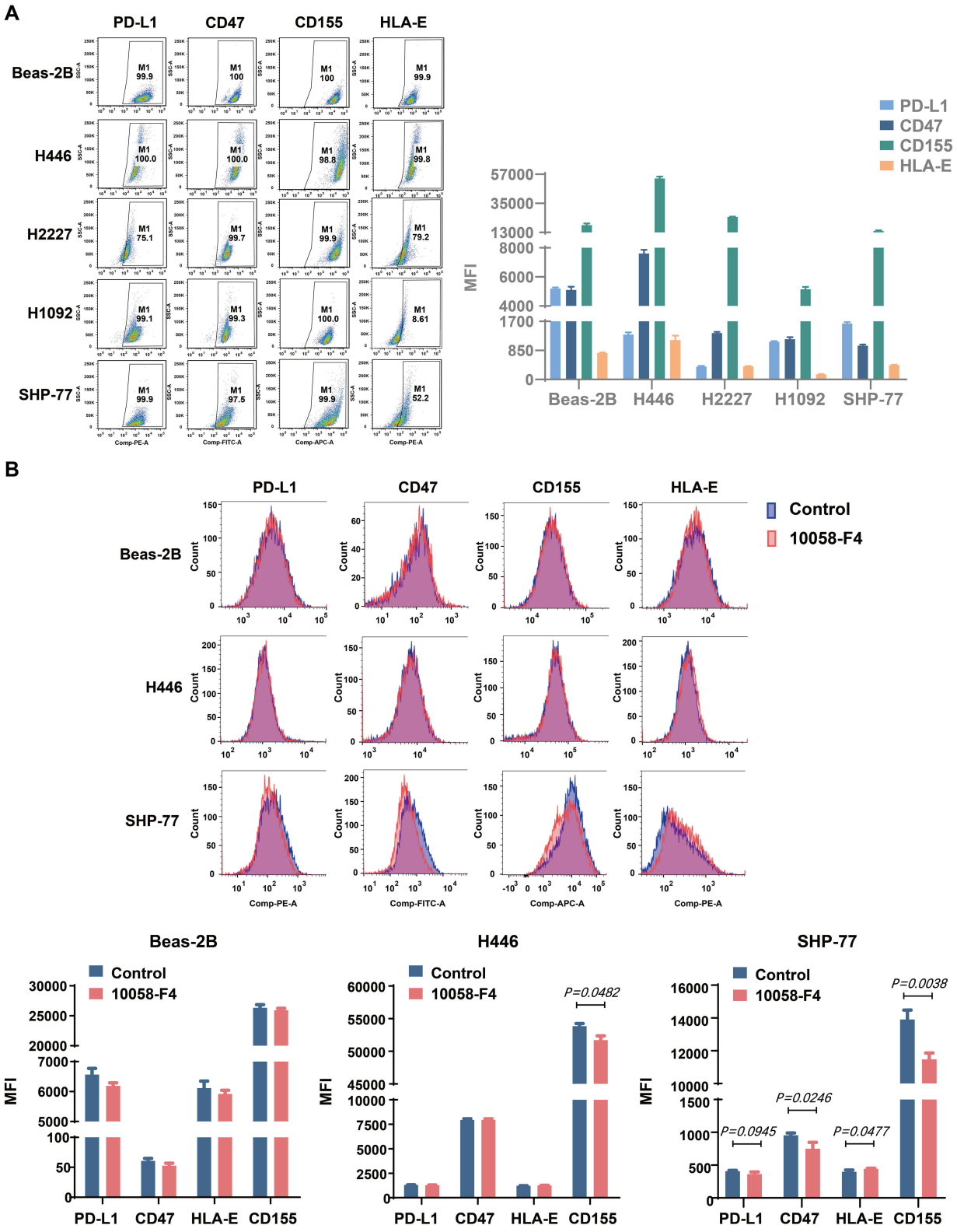

Fig. 3. Expression levels of PD-L1, CD47, HLA-E, and CD155 on the surface of cells treated or not treated with 10058-F4. (A) Flow cytometry results of the expression levels of PD-L1, CD47, HLA-E, and CD155 on different cells, including Beas-2B, H446, H2227, H1092, and SHP-77 cells. (B) Expression levels of PD-L1, CD47, HLA-E, and CD155 on Beas-2B, H446 and SHP-77 cells with or without 10058-F4 treatment. Data are presented as mean ± standard deviation from three independent experiments and analyzed by Student's two-tailed *t*-tests. PD-L1, programmed death ligand 1; HLA-E, human leukocyte antigen-E; MFI, mean fluorescence intensity.

sion levels of immunosuppressive ligands on the surface of Beas-2B cells were not significantly altered by treatment with 10058-F4.

3.3 Effect of c-Myc Expression in SCLC Cells on the Function of Immune Cells

To investigate the regulatory effect of c-Myc expression in SCLC cells on the immune microenvironment, SCLC cells with or without 10058-F4 treatment were cocultured with T cells and THP-1-derived macrophages, and CD3 expression levels, IFN-γ levels in the supernatant, and phagocytosis percentages were determined. The percentage of Jurkat cells and the expression level of CD3 thereon in the 10058-F4 group were not different from those in the control group (Fig. 4A,B). The IFN-γ concentration in the supernatant of the H446 coculture system in the 10058-F4 group significantly exceeded that in the control group (p = 0.0055), whereas no such difference was observed for the supernatant of the SHP-77 coculture system (Fig. 4C). 10058-F4 significantly downregulated phagocytosis by THP-1-derived macrophages cocultured with SHP-77 and H446 cells but not Beas-2B cells (Fig. 4D). IL-6 and IL-10 concentrations in the supernatant were decreased for the H446 cells + macrophage coculture system in the 10058-F4 group, whereas there was a trend of downregulation was observed in the SHP-77 cell coculture system (Fig. 4E). These results imply that c-Myc inhibition in SCLC cells can significantly upregulate IFN-γ production by T cells but inhibit phagocytosis by macrophages and decrease IL-6 and IL-10 concentrations.

3.4 Regulatory Effect of c-Myc on β-Catenin Expression

Based on the interaction between c-Myc and the Notch signaling pathway [10], we measured the expression levels of related molecules in the latter pathway in Beas-2B, H446, and SHP-77 cells with or without 10058-F4 treatment. Notch1, cleaved-Notch1, RBPSUH, and P21 levels were changed by 10058-F4 in SCLC cells (Fig. 5A), which confirmed that 10058-F4 regulated the Notch signaling pathway in these cells. Additionally, 10058-F4 inhibited the expression of E- and VE-cadherins (Fig. 5B), the hallmarks of the epithelial–mesenchymal transition [19], which confirmed the regulatory effect of c-Myc on this transition in SCLC cells. Given that the Notch signaling pathway regulates the immune microenvironment of hepatocellular carcinoma through WNT signaling [20], we quantified β-catenin expression in Beas-2B and SCLC cells with or without 10058-F4 treatment. 10058-F4 significantly downregulated β-catenin expression (Fig. 5C) and could therefore regulate the WNT/β-catenin pathway in SCLC cells.

3.5 Effect of a β-Catenin Agonist on the Regulatory Effect of 10058-F4 on Suppressor Ligands in SCLC Cells

To determine whether c-Myc inhibition regulates the expression of immunosuppressive ligands on SCLC cells through the WNT/β-catenin pathway, we determined the concentrations of SKL2001—a β-catenin agonist—sufficient to upregulate the expression of β-catenin in Beas-2B, H446, and SHP-77 cells. These concentrations were 5 μM for Beas-2B and H446 cells and 20 μM for SHP-77 cells (Fig. 6A), and the optimal working concentrations were set accordingly. Subsequently, we treated Beas-2B, H446, and SHP-77 cells with 10058-F4, SKL2001, and a combination of 10058-F4 and SKL2001 for 48 h. SKL2001 increased the MFI of PD-L1, CD47, and HLA-E on H446 cells and recovered the MFI of the above ligands, which were downregulated by 10058-F4 (Fig. 6C). In SHP-77 cells, SKL2001 significantly recovered the MFIs of CD155, which were downregulated by 10058-F4 (Fig. 6D). However, only PD-L1 was markedly regulated, while other immunosuppressive ligands on Beas-2B cells were not significantly altered (Fig. 6B). Thus, c-Myc may modulate the expression of immunosuppressive ligands through the WNT/β-catenin signaling pathway in SCLC cells.

4. Discussion

SCLC is an immune-cold tumor with few infiltrated cytotoxic lymphocytes and one-fifth of the total immune cells compared with non-small cell lung cancer (NSCLC) [21] and exhibits more pronounced immune exclusion and less pronounced immune invasion than lung adenocarcinoma [22], which could explain the limited efficacy of immunotherapy in SCLC. Relevant study demonstrated that c-Myc regulates the evolution of SCLC from a NE phenotype with less immune infiltration to a non-NE phenotype with more immune infiltration [10], highlighting the regulatory effect of c-Myc on the immune microenvironment of SCLC [23]. Herein, c-Myc expression was found to be positively correlated with immune infiltration, especially the $CD163^+$ macrophages in SCLC. c-Myc inhibition significantly altered the expression of immunosuppressive ligands—including PD-L1, CD47, HLA-E, and CD155—on SCLC cells, as well as the secretion of IL-6, IL-10, and GM-CSF, which was probably regulated by the WNT/β-catenin pathway (Fig. 7). The results provide reliable evidence for understanding the immune characteristics, key molecules, and mechanisms regulating immune signatures in SCLC. Chen et al. identified IL-27RA as an immune regulator and therapeutic marker for breast cancer through transcriptomic and single-cell analysis [24].

The composition of immune cells strongly influences tumor progression and immune evasion [25]. TILs are primarily classified as T lymphocytes, B lymphocytes, macrophages, and NK cells. The most infiltrating TILs in SCLC are T cells and monocytes [22]. Based on their polarization and activation markers, macrophages are classified as M1 and M2, with the former phenotype accelerating the inflammatory response and the latter decelerating it. After being recruited to tumor tissues via numerous signals in the tumor microenvironment, monocytes even-

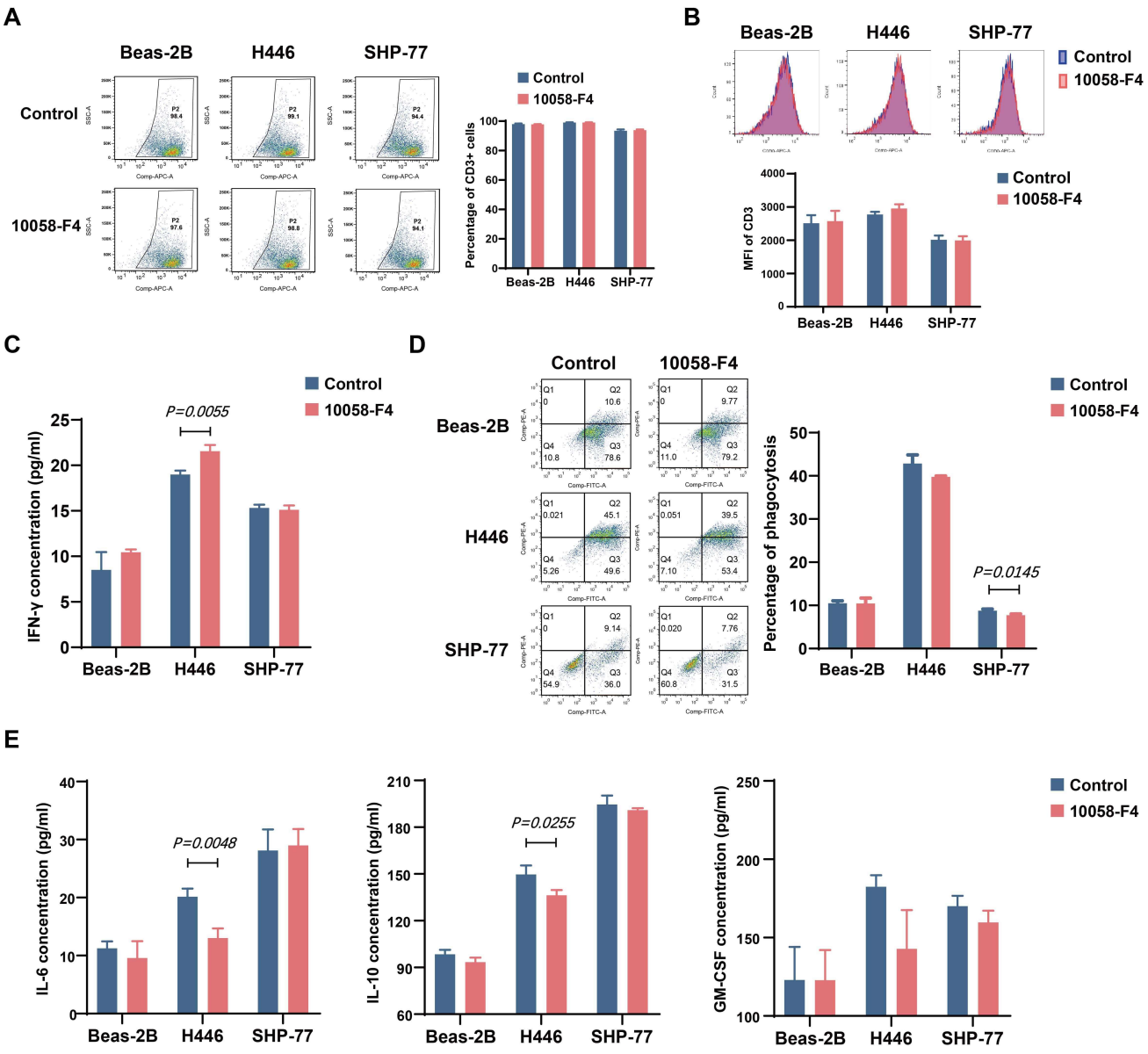

Fig. 4. Regulatory effect of 10058-F4 on the function of T cells and macrophages cocultured with SCLC cells. (A) Percentages of $CD3^+$ T cells in the coculture systems of Jurkat and Beas-2B or SCLC cells with or without 10058-F4 treatment. (B) CD3 expression levels on Jurkat cells cocultured with Beas-2B or SCLC cells with or without 10058-F4 treatment. (C) IFN-γ concentrations in the supernatant of the coculture system of Jurkat cells and Beas-2B or SCLC cells with or without 10058-F4 treatment. (D) Phagocytosis percentages of THP-1-derived macrophages and (E) concentrations of IL-6, IL-10, and GM-CSF in the supernatant of macrophages + Beas-2B or SCLC cell coculture system. Data are presented as mean ± standard deviation from three independent experiments and analyzed by Student's two-tailed *t*-tests. IFN-γ, interferon-gamma; IL-6, interleukin-6; IL-10, interleukin-10; GM-CSF, granulocyte-macrophage colony-stimulating factor.

tually develop into tumor-associated macrophages, which are considered M2 macrophages [26] and are significantly associated with the recurrence of SCLC [22]. Herein, the high expression of c-Myc was significantly positively correlated with M2 macrophage infiltration. As an inhibitory signal for macrophages, CD47 is often overexpressed on cancer cells [27], interacts with SIRPα, and initiates a signaling cascade to inhibit phagocytosis. However, c-Myc inhibition significantly downregulated CD47 expression on SCLC cells while weakening their phagocytosis by THP-1-derived macrophages. This finding may be due to the downregulated expression of GM-CSF—a potent macrophage activator [28]—by c-Myc inhibition in SCLC.

The infiltration of $CD8^+$ T cells was reported to be more pronounced in the inflammatory subtype/non-NE phenotype SCLC [29] and is known to be associated with

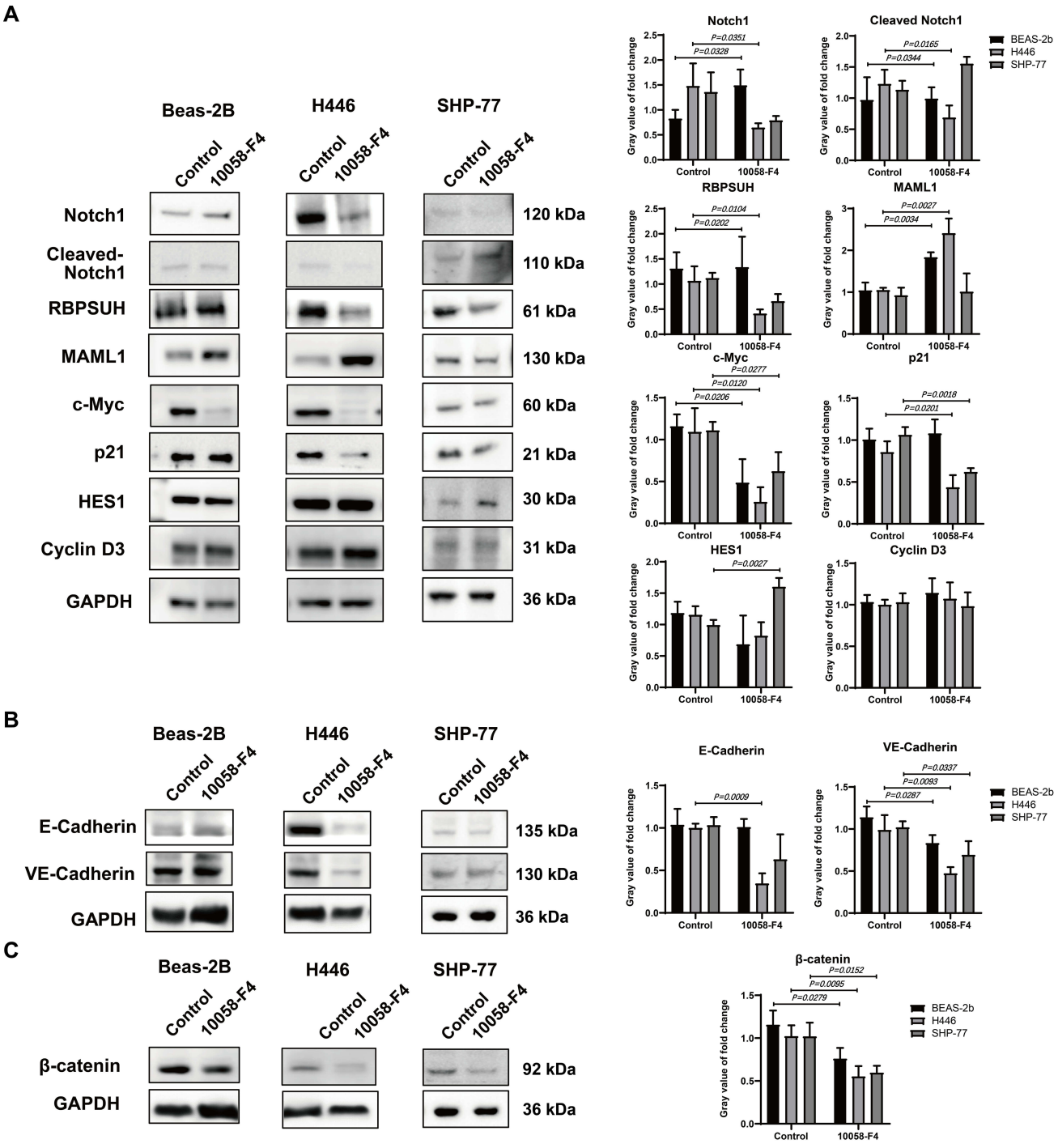

Fig. 5. Effect of 10058-F4 on Notch signaling, epithelial–mesenchymal transition, and β-catenin expression. (A) Expression levels of key molecules in Notch signaling (including Notch1, cleaved Notch1, RBPSUH, MAML1, c-Myc, p21, HES1, and Cyclin D3) in Beas-2B, H446, and SHP-77 cells with or without 10058-F4 treatment. (B) E-cadherin and VE-cadherin expression levels in Beas-2B, H446, and SHP-77 cells in control and 10058-F4 groups. (C) β-Catenin expression levels in Beas-2B, H446, and SHP-77 cells in control and 10058-F4 groups. VE, vascular endothelial.

the efficacy of SCLC immunotherapy [30]. However, we observed no significant correlation between c-Myc expression and the level of $CD8^+$ T cell infiltration. Although IFN-γ was upregulated in the coculture system after the inhibition of c-Myc in H446 cells, Jurkat cells were not activated. This behavior may be attributed to the upregulation of other immunosuppressive ligands, including LAG3 and CTLA-4, on H446 cells, which counteracted the effect of IFN-γ on Jurkat cells. Conversely, c-Myc suppression in SHP-77 cells downregulated surface CD155 expression,

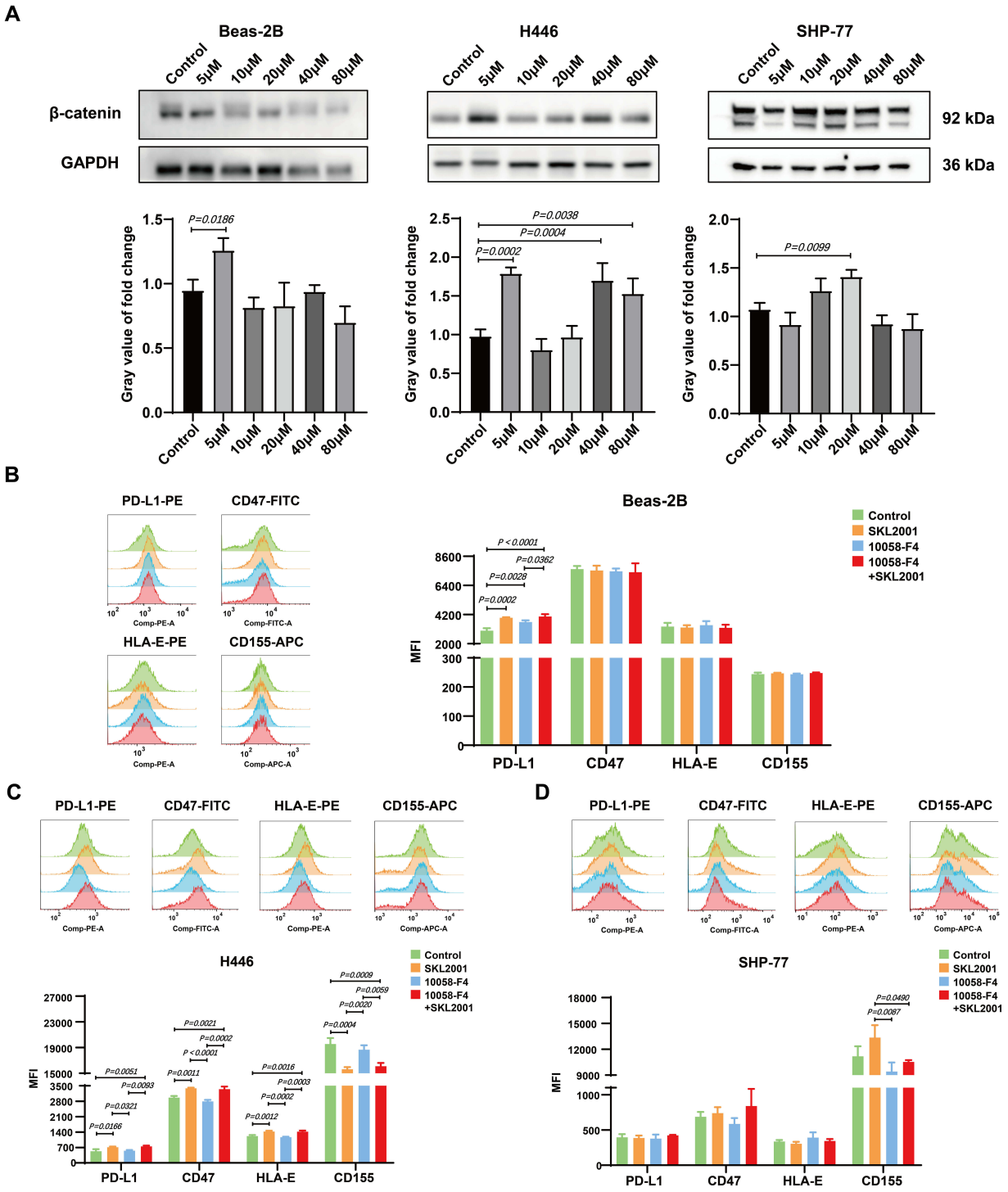

Fig. 6. Effect of SKL2001 on β-catenin expression and that of 10058-F4 on immunosuppressive ligands. (A) Expression levels of β-catenin in Beas-2B, H446, and SHP-77 cells treated with different concentrations of SKL2001. MFIs of immunosuppressive ligands (PD-L1, CD47, HLA-E, and CD155) on (B) Beas-2B, (C) H446, and (D) SHP-77 cells treated with SKL2001, 10058-F4, or 10058-F4 combined with SKL2001. Data are presented as mean ± standard deviation from three independent experiments and analyzed by Student's two-tailed *t*-tests.

potentially because of SCLC lineage heterogeneity. SCLC-A and SCLC-Y subtypes [10] exhibit different cellular origins [31] and intrinsic regulatory programs [32], thus featuring divergent immune checkpoint expression [18]. This implies that $CD8^+$ T cell infiltration is regulated by additional key molecules, a premise that requires further investigation.

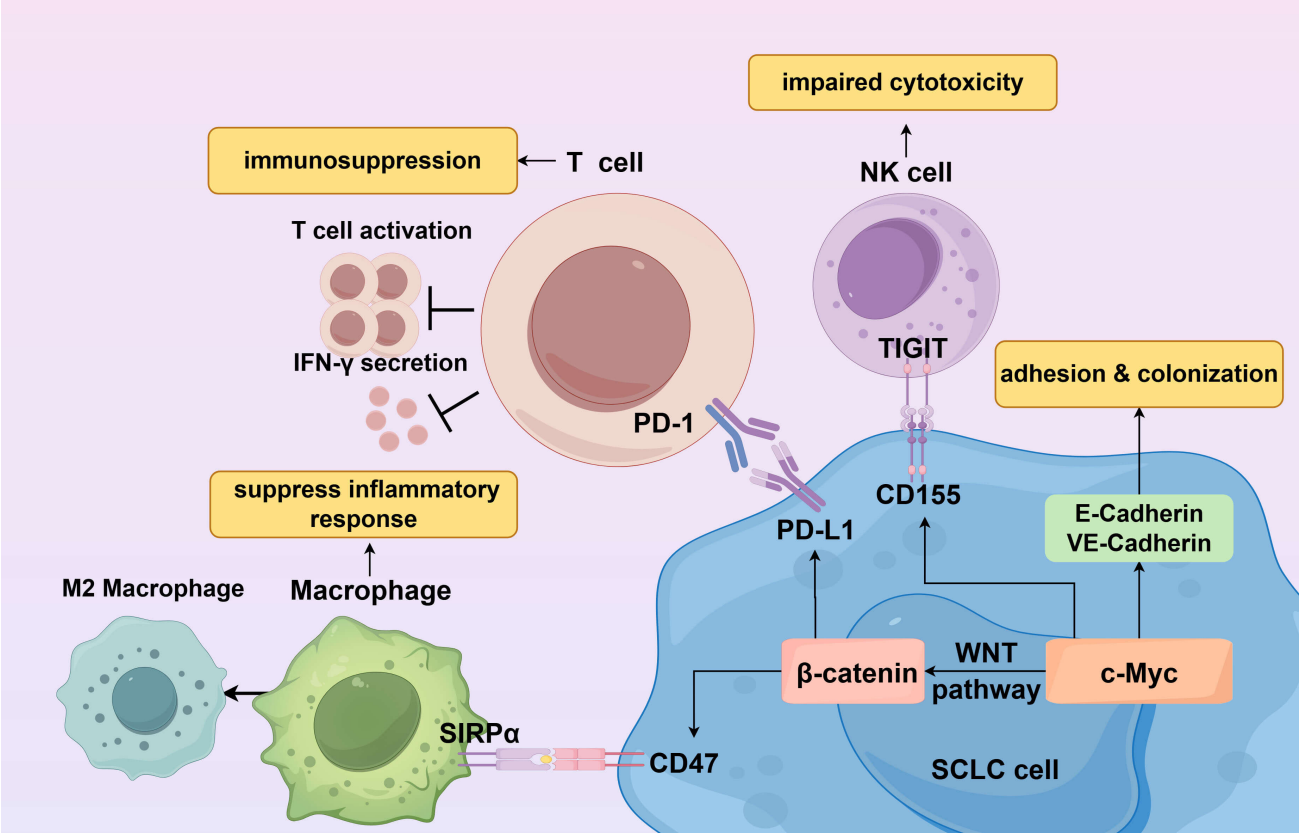

Fig. 7. Schematic of the regulatory effects of c-Myc on immunosuppressive ligands in SCLC. In SCLC, c-Myc expression regulates the cell surface expression levels of PD-L1, CD155, and CD47 via the WNT/β-catenin signaling pathway. CD155 binds to TIGIT on the surface of natural killer cells, impairing their cytotoxicity. PD-L1 interacts with PD-1 on immune cells such as T cells, causing T cell immunosuppression. CD47 binds to SIRPα on the surface of macrophages, promoting macrophage differentiation toward the M2 phenotype and thereby suppressing inflammatory responses. Additionally, c-Myc is involved in regulating VE- and E-cadherins, which are hallmarks of cell adhesion, colonization, and the epithelial–mesenchymal transition. NK, natural killer; TIGIT, T cell immunoreceptor with Ig and ITIM domains; SIRPα, signal regulatory protein α. The schematic figure was drawn via Figdraw (Hangzhou, Zhejiang, China).

Our findings, based on the analysis of tumor tissues from 24 patients with LS-SCLC, provide a potential rationale for the earlier incorporation of immunotherapy in LS-SCLC, which is currently confined to consolidation maintenance [33]. Patients with high tumor c-Myc expression may exhibit elevated levels of immune checkpoints, which can limit the efficacy of ICI monotherapy. In such cases, the application of β-catenin inhibitors or combination ICI therapy might effectively suppress the c-Myc-regulated immune checkpoint pathway, reactivate immune cells, and improve the response to ICI treatment. Consequently, c-Myc may serve as a potential biomarker for guiding combination immunotherapy in LS-SCLC. This concept is supported by similar studies on breast cancer, such as an mGPS-based prediction study, which highlights the importance of immune-nutritional markers as clinical predictors [34]. In the more prevalent and aggressive ES-SCLC, validating the correlation between c-Myc and immune cells, as well as the regulatory mechanisms in ES-SCLC samples, would improve the predictive value of c-Myc for combination immunotherapy and enable its extension to a broader patient population. The absence of such validation represents a notable limitation of this study and a key direction for future research on ES-SCLC.

5. Limitation

The correlation between c-Myc and immune cells was identified using tissue samples from a small cohort of patients with LS-SCLC. Future studies should validate these findings using larger cohorts of LS-SCLC and ES-SCLC patient samples to capture tumor characteristics across all stages of SCLC and examine the generalizability of this correlation. Furthermore, the regulatory relationships in this study were established using *in vitro* cell lines. Additional validation in models better recapitulating the human tumor microenvironment, such as organoids or humanized mouse models, is needed to advance the development of targeted therapies for SCLC.

6. Conclusions

c-Myc inhibits the function of NK cells and macrophages, exerting a regulatory effect on the immune microenvironment in SCLC. This result validates our hypothesis in the tumor tissues of patients with SCLC and proves that the regulatory effect of c-Myc on different immune-related ligands is exerted through the WNT signaling pathway. The obtained reliable evidence is suitable for elucidating the characteristics and formation mechanism of immune-cold tumors in SCLC and establishing a new direction for the study of biomarkers and new targets for SCLC immunotherapy.

Availability of Data and Materials

The datasets used or analyzed during the current study are available from the corresponding author on reasonable request.

Author Contributions

PYZ and HFL designed the research study, PYZ, HL and XYW performed the research, ND and YL participated in experiments, LT, RZ and CLL analyzed the data, PYZ wrote the initial draft. All authors contributed to editorial changes in the manuscript. All authors read and approved the final manuscript. All authors have participated sufficiently in the work and agreed to be accountable for all aspects of the work.

Ethics Approval and Consent to Participate

This study was approved by the Ethics Committee of Jilin Cancer Hospital, China (202102-03-01). Informed patient consent was obtained prior to tissue collection. All procedures complied with the relevant regulations and the Declaration of Helsinki.

Acknowledgment

Not applicable.

Funding

This work was supported by Jilin Provincial Department of Science and Technology (YDZJ202201ZYTS168), China Association for Science and Technology (QT202218) and National Natural Science Foundation of China (82103343).

Conflicts of Interest

The authors declare no conflicts of interest.

Supplementary Material

Supplementary material associated with this article can be found, in the online version, at https://doi.org/10.31083/FBL52899.

References

[1] Filho AM, Laversanne M, Ferlay J, Colombet M, Piñeros M, Znaor A, et al. The GLOBOCAN 2022 cancer estimates: Data sources, methods, and a snapshot of the cancer burden worldwide. International Journal of Cancer. 2025; 156: 1336–1346. https://doi.org/10.1002/ijc.35278

[2] Früh M, De Ruysscher D, Popat S, Crinò L, Peters S, Felip E, et al. Small-cell lung cancer (SCLC): ESMO Clinical Practice Guidelines for diagnosis, treatment and follow-up. Annals of Oncology: Official Journal of the European Society for Medical Oncology. 2013; 24: vi99–vi105. https://doi.org/10.1093/annonc/mdt178

[3] Gazdar AF, Bunn PA, Minna JD. Small-cell lung cancer: what we know, what we need to know and the path forward. Nature Reviews. Cancer. 2017; 17: 725–737. https://doi.org/10.1038/nrc.2017.87

[4] Sen T, Takahashi N, Chakraborty S, Takebe N, Nassar AH, Karim NA, et al. Emerging advances in defining the molecular and therapeutic landscape of small-cell lung cancer. Nature Reviews. Clinical Oncology. 2024; 21: 610–627. https://doi.org/10.1038/s41571-024-00914-x

[5] Sabari JK, Lok BH, Laird JH, Poirier JT, Rudin CM. Unravelling the biology of SCLC: implications for therapy. Nature Reviews. Clinical Oncology. 2017; 14: 549–561. https://doi.org/10.1038/nrclinonc.2017.71

[6] Liu SV, Reck M, Mansfield AS, Mok T, Scherpereel A, Reinmuth N, et al. Updated Overall Survival and PD-L1 Subgroup Analysis of Patients With Extensive-Stage Small-Cell Lung Cancer Treated With Atezolizumab, Carboplatin, and Etoposide (IMpower133). Journal of Clinical Oncology: Official Journal of the American Society of Clinical Oncology. 2021; 39: 619–630. https://doi.org/10.1200/JCO.20.01055

[7] Paz-Ares L, Dvorkin M, Chen Y, Reinmuth N, Hotta K, Trukhin D, et al. Durvalumab plus platinum-etoposide versus platinum-etoposide in first-line treatment of extensive-stage small-cell lung cancer (CASPIAN): a randomised, controlled, open-label, phase 3 trial. Lancet (London, England). 2019; 394: 1929–1939. https://doi.org/10.1016/S0140-6736(19)32222-6

[8] Das SK, Lewis BA, Levens D. MYC: a complex problem. Trends in Cell Biology. 2023; 33: 235–246. https://doi.org/10.1016/j.tcb.2022.07.006

[9] Casey SC, Baylot V, Felsher DW. The MYC oncogene is a global regulator of the immune response. Blood. 2018; 131: 2007–2015. https://doi.org/10.1182/blood-2017-11-742577

[10] Ireland AS, Micinski AM, Kastner DW, Guo B, Wait SJ, Spainhower KB, et al. MYC Drives Temporal Evolution of Small Cell Lung Cancer Subtypes by Reprogramming Neuroendocrine Fate. Cancer Cell. 2020; 38: 60–78.e12. https://doi.org/10.1016/j.ccell.2020.05.001

[11] Kanemura H, Hayashi H, Tomida S, Tanizaki J, Suzuki S, Kawanaka Y, et al. The Tumor Immune Microenvironment and Frameshift Neoantigen Load Determine Response to PD-L1 Blockade in Extensive-Stage SCLC. JTO Clinical and Research Reports. 2022; 3: 100373. https://doi.org/10.1016/j.jtocrr.2022.100373

[12] Alburquerque-Bejar JJ, Navajas-Chocarro P, Saigi M, Ferrero-Andres A, Morillas JM, Vilarrubi A, et al. MYC activation impairs cell-intrinsic IFNγ signaling and confers resistance to anti-PD1/PD-L1 therapy in lung cancer. Cell Reports. Medicine. 2023; 4: 101006. https://doi.org/10.1016/j.xcrm.2023.101006

[13] Zhao P, Sun X, Li H, Liu Y, Cui Y, Tian L, et al. c-Myc Targets HDAC3 to Suppress NKG2DL Expression and Innate Immune Response in N-Type SCLC through Histone Deacetylation. Cancers. 2022; 14: 457. https://doi.org/10.3390/cancers14030457

[14] Tian L, Li H, Zhao P, Liu Y, Lu Y, Zhong R, et al. C-Myc-induced hypersialylation of small cell lung cancer facilitates pro-tumoral

phenotypes of macrophages. IScience. 2023; 26: 107771. https://doi.org/10.1016/j.isci.2023.107771

[15] Liu JX, Lu T, Xia Y, Yang J, Jiang YF, Zhao Y, et al. Expression and correlation of Surfeit 4 gene in esophageal squamous cell carcinoma. Holistic Integrative Oncology. 2024; 3: 66. https://doi.org/10.1007/s44178-024-00141-5

[16] Denkert C, von Minckwitz G, Darb-Esfahani S, Lederer B, Heppner BI, Weber KE, et al. Tumour-infiltrating lymphocytes and prognosis in different subtypes of breast cancer: a pooled analysis of 3771 patients treated with neoadjuvant therapy. The Lancet. Oncology. 2018; 19: 40–50. https://doi.org/10.1016/S1470-2045(17)30904-X

[17] Rudin CM, Poirier JT, Byers LA, Dive C, Dowlati A, George J, et al. Molecular subtypes of small cell lung cancer: a synthesis of human and mouse model data. Nature Reviews. Cancer. 2019; 19: 289–297. https://doi.org/10.1038/s41568-019-0133-9

[18] Gay CM, Stewart CA, Park EM, Diao L, Groves SM, Heeke S, et al. Patterns of transcription factor programs and immune pathway activation define four major subtypes of SCLC with distinct therapeutic vulnerabilities. Cancer Cell. 2021; 39: 346–360.e7. https://doi.org/10.1016/j.ccell.2020.12.014

[19] Russo GC, Crawford AJ, Clark D, Cui J, Carney R, Karl MN, et al. E-cadherin interacts with EGFR resulting in hyper-activation of ERK in multiple models of breast cancer. Oncogene. 2024; 43: 1445–1462. https://doi.org/10.1038/s41388-024-03007-2

[20] Ye YC, Zhao JL, Lu YT, Gao CC, Yang Y, Liang SQ, et al. NOTCH Signaling via WNT Regulates the Proliferation of Alternative, CCR2-Independent Tumor-Associated Macrophages in Hepatocellular Carcinoma. Cancer Research. 2019; 79: 4160–4172. https://doi.org/10.1158/0008-5472.CAN-18-1691

[21] Busch SE, Hanke ML, Kargl J, Metz HE, MacPherson D, Houghton AM. Lung Cancer Subtypes Generate Unique Immune Responses. Journal of Immunology (Baltimore, Md.: 1950). 2016; 197: 4493–4503. https://doi.org/10.4049/jimmunol.1600576

[22] Chan JM, Quintanal-Villalonga Á, Gao VR, Xie Y, Allaj V, Chaudhary O, et al. Signatures of plasticity, metastasis, and immunosuppression in an atlas of human small cell lung cancer. Cancer Cell. 2021; 39: 1479–1496.e18. https://doi.org/10.1016/j.ccell.2021.09.008

[23] Nirala BK, Yustein JT. The Role of MYC in Tumor Immune Microenvironment Regulation: Insights and Future Directions. Frontiers in Bioscience (Landmark Edition). 2025; 30: 37304. https://doi.org/10.31083/FBL37304

[24] Chen Y, Anwar M, Wang X, Zhang B, Ma B. Integrative transcriptomic and single-cell analysis reveals IL27RA as a key immune regulator and therapeutic indicator in breast cancer. Discover Oncology. 2025; 16: 977. https://doi.org/10.1007/s12672-025-02811-w

[25] Li K, Zeng X, Zhang Z, Wang K, Pan Y, Wu Z, et al. Pan-immune-inflammatory values predict survival in patients after radical surgery for non-metastatic colorectal cancer: A retrospective study. Oncology Letters. 2025; 29: 197. https://doi.org/10.3892/ol.2025.14943

[26] Cassetta L, Pollard JW. Tumor-associated macrophages. Current Biology: CB. 2020; 30: R246–R248. https://doi.org/10.1016/j.cub.2020.01.031

[27] van Duijn A, Van der Burg SH, Scheeren FA. CD47/SIRPα axis: bridging innate and adaptive immunity. Journal for Immunotherapy of Cancer. 2022; 10: e004589. https://doi.org/10.1136/jitc-2022-004589

[28] Zhang S, Rautela J, Bediaga NG, Kolesnik TB, You Y, Nie J, et al. CIS controls the functional polarization of GM-CSF-derived macrophages. Cellular & Molecular Immunology. 2023; 20: 65–79. https://doi.org/10.1038/s41423-022-00957-z

[29] Qu S, Fetsch P, Thomas A, Pommier Y, Schrump DS, Miettinen MM, et al. Molecular Subtypes of Primary SCLC Tumors and Their Associations With Neuroendocrine and Therapeutic Markers. Journal of Thoracic Oncology: Official Publication of the International Association for the Study of Lung Cancer. 2022; 17: 141–153. https://doi.org/10.1016/j.jtho.2021.08.763

[30] Sen T, Rodriguez BL, Chen L, Corte CMD, Morikawa N, Fujimoto J, et al. Targeting DNA Damage Response Promotes Antitumor Immunity through STING-Mediated T-cell Activation in Small Cell Lung Cancer. Cancer Discovery. 2019; 9: 646–661. https://doi.org/10.1158/2159-8290.CD-18-1020

[31] Solta A, Ernhofer B, Boettiger K, Megyesfalvi Z, Heeke S, Hoda MA, et al. Small cells - big issues: biological implications and preclinical advancements in small cell lung cancer. Molecular Cancer. 2024; 23: 41. https://doi.org/10.1186/s12943-024-01953-9

[32] Tenjin Y, Matsuura K, Kudoh S, Usuki S, Yamada T, Matsuo A, et al. Distinct transcriptional programs of SOX2 in different types of small cell lung cancers. Laboratory Investigation; a Journal of Technical Methods and Pathology. 2020; 100: 1575–1588. https://doi.org/10.1038/s41374-020-00479-0

[33] Cheng Y, Spigel DR, Cho BC, Laktionov KK, Fang J, Chen Y, et al. Durvalumab after Chemoradiotherapy in Limited-Stage Small-Cell Lung Cancer. The New England Journal of Medicine. 2024; 391: 1313–1327. https://doi.org/10.1056/NEJMoa2404873

[34] Chen Y, Zhang B, Wang X, Chen Y, Anwar M, Fan J, et al. Prognostic value of preoperative modified Glasgow prognostic score in predicting overall survival in breast cancer patients: A retrospective cohort study. Oncology Letters. 2025; 29: 180. https://doi.org/10.3892/ol.2025.14926